Effect of quenching in resonant coherent excitation of hydrogen atoms scattered from LiF surfaces

A. V. Lugovskoy* and I. Bray†
Centre for Atomic, Molecular and Surface Physics, School of Mathematical and Physical Sciences, Murdoch University, Perth 6150, Australia
(Received 5 November 2002; published 10 March 2003)

In this paper we analyze theoretically the ''signal background'' observed in experimental studies of the radiative decay of hydrogen atoms following resonant coherent excitation (RCE) in grazing collisions with a LiF surface. The radiation intensity is evaluated by treating the RCE within a time-dependent (classical-trajectory) quantal approach, and by assuming that the excited electronic states are quenched whenever the atom-surface distance drops below a certain ''switching distance.'' Associating the mechanism of excited-state quenching with the charge transfer to the LiF conduction band we show that the hereto unexplained signal background can be attributed to the dependence of the switching distance on the incident energy.

DOI: 10.1103/PhysRevA.67.032901 PACS number(s): 79.20.Rf, 03.65.Nk, 61.12.Bt

I. INTRODUCTION

Investigation of elementary interactions on solid surfaces initiated by particle beams has been of significant scientific and practical interest for a long time. The last two decades witnessed rapid progress in the field in both experimental techniques and theoretical methods [1–6].

One of the new developments in this field is the resonant coherent excitation (RCE) of atomic projectiles in grazing scattering from insulator surfaces [7]. The RCE takes place when a projectile travels through or near a spatially periodic structure with velocity $V=\omega d/2\pi$, where ω is some characteristic electron excitation frequency of the projectile and d is a structure constant. In this case the projectile experiences a periodic-in-time resonant perturbation resulting in projectile excitation. More detail, historical insight, and references to the topic can be found in the review of Winter [4].

Our specific interest is the RCE of a hydrogen atom scattering at grazing angles from a lithium fluoride surface. The RCE effect for this system was first observed by Auth *et al.* [7]. Measuring the intensity of the Lyman-α light as a function of the initial projectile energy, they detected a pronounced resonant structure on top of a nonresonant asymmetric background. Subsequently, with the use of the projectile-photon coincidence technique, it was shown that this background could be significantly reduced, but it did not vanish [8]. It was also found that the peak position of the resonance is shifted towards larger energies [7,8].

The physical reasons causing the background formation in the observed signal have not yet been identified. Auth and Winter [8] supposed that it might be a kinematically enhanced electron-capture mechanism resulting in the extra population of the excited outgoing hydrogen atom. For the shift in the signal peak position, it was suggested that the RCE switches on when the atom is sufficiently far from the surface in the outgoing part of its trajectory with no further significant energy loss [7,8]. This interpretation is based on the viewpoint that the lifetimes of the hydrogen excited states are strongly reduced in the vicinity of the surface.

The mechanisms leading to effective quenching of the excited electronic states are also not completely understood. Since the direct transfer of the hydrogen electron excitation to electrons in the solid is unlikely in the wide-band-gap insulators, the presumably binary collision types of interaction mechanisms (electron promotion by formation of molecular orbitals, etc.) were suggested to be responsible for quenching [8]. However, as shown by Zeijlmans van Emmichoven *et al.* [9], the electron promotion followed by molecular autoionization works for incident energies between 100 eV and 1 keV. The energy range in the RCE experiment stretches from 4 keV to 8 keV. In this region the atom is too fast for its electron to form molecules with F^- sites of the lattice.

To get more insight into the behavior of the system, we analyze the influence of the kinematic factors, such as different trajectories for different projectile energies and projectile deceleration during the collision, on the RCE signal. We also study how the signal depends on the distance Z_{sw} above which RCE is possible with no quenching of the atom excitation. In addition, we consider the situation where quenching is negligible throughout the trajectory and hence RCE is possible in the incoming part of the trajectory.

In this work we suggest an interpretation of the observed RCE signal background. Considering the case where the switching distance is a function of the initial projectile energy $[Z_{sw}\equiv Z_{sw}(E_i)]$ one can reproduce, to a large extent, the signal shape close to that observed in the experiment. The energy dependence follows from the quenching mechanism of the excited states. In our work we assume that this mechanism is of the charge-transfer type from excited states of hydrogen to the LiF conduction band. Under the conditions typical in the RCE experiments, this charge-transfer process can be significantly kinematically enhanced. In our model, the signal background appears as a result of the deterministic evolution of the excited-state populations and no additional mechanism is needed for its formation.

II. THEORETICAL MODEL

Following the experimental setup of Auth and Winter [8], we have a proton of initial energy E_i directed to a LiF surface under a grazing angle ϕ_i (the angle between the initial

*Electronic address: andrey@atom.murdoch.edu.au
†Electronic address: I.Bray@murdoch.edu.au

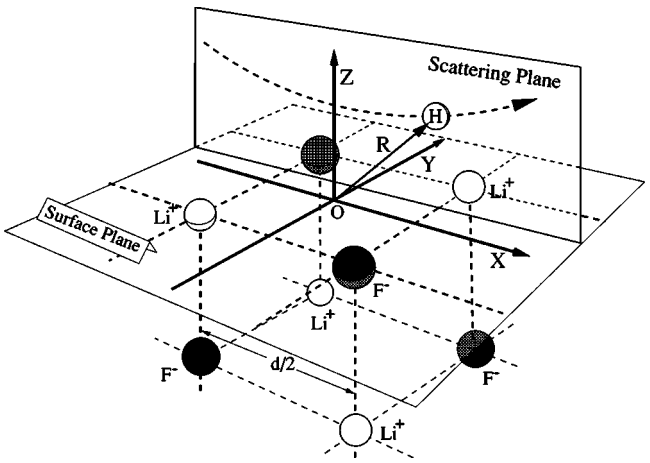

FIG. 1. Sketch of scattering geometry for collisions of hydrogen atoms from a LiF surface at glancing angle of incidence.

projectile velocity and the surface plane) (see Fig. 1).

Exposed to the self-induced image force, the incoming proton accumulates some additional energy $E_{\rm im}$ until it forms neutral H at a distance Z_n due to electron capture from the insulator valence band to the $1s$ state. The behavior of the atom-insulator system in the very vicinity of the surface can be very complicated. This is due to the combined action of resonant electron interaction with the surface and the following quenching of the excited atomic states. If mechanisms such as atomic electron promotion followed by ionization come forward in this phase of the process, one can expect a series of reionization-reneutralization cycles for the projectile. To describe this phase in the system evolution, one needs to solve the multielectron problem.

In this paper we restrict our consideration only to the phase where RCE is possible, that is, for $Z>Z_{\rm sw}$. Below $Z_{\rm sw}$ only the $1s$ state is assumed to be stable and, hence, no RCE is allowed.

For the process phase of interest, the atom excitation can be found from the solution of the Schrödinger equation

$$i\frac{\partial\psi(\boldsymbol{r},t)}{\partial t}=\left[-\frac{\Delta_{\boldsymbol{r}}}{2}+V_a(\boldsymbol{r})+V_s(\boldsymbol{r}+\boldsymbol{R}(t))\right]\psi(\boldsymbol{r},t), \quad (1)$$

where $\Delta_{\boldsymbol{r}}=\partial^2/\partial x^2+\partial^2/\partial y^2+\partial^2/\partial z^2$, ψ is the atomic electron wave function, $V_a(\boldsymbol{r})=-1/r$ and $V_s(\boldsymbol{r})$ are, respectively, the electron-proton and electron-lattice interactions, and $\boldsymbol{R}(t)$ is the position of the proton with respect to the lattice, see Fig. 1. We assume that the atom is in the $1s$ state at $Z=Z_{\rm sw}$. Atomic units are used throughout unless specified otherwise.

To solve Eq. (1) the wave function is expanded over the atomic orbitals φ_n of energy ε_n,

$$\psi(\boldsymbol{r},t)=\sum_n a_n(t)\varphi_n(\boldsymbol{r})\exp[-i\varepsilon_n t]. \quad (2)$$

Subscript n in Eq. (2) stands for the full set of quantum numbers. Here we use the spherical harmonic decomposition of the wave function (2) so that $n\equiv\{n,l,m\}$.

The atom trajectory is determined by the position of the hydrogen mass center $\boldsymbol{R}(t)=(X(t),Y,Z(t))$. The experiment in Ref. [8] has the projectile propagating along the [100] direction of the LiF crystal (x direction). The z axis is chosen to be normal to the surface. The reference frame origin is placed on the first layer of the crystal as shown in Fig. 1.

In our calculations we find $\boldsymbol{R}(t)$ numerically by solving the classical equations of motion

$$M\frac{d^2\boldsymbol{R}(t)}{dt^2}=\boldsymbol{F}(Z(t)), \quad (3)$$

where the force

$$\boldsymbol{F}(Z)=-\frac{dE}{dX}(Z)\hat{x}-\frac{dU}{dZ}\hat{z} \quad (4)$$

is a sum of a stopping power $-dE/dX$ and a term due to the atom-surface repulsion [$U(Z)$ is a planar atom-surface potential]. In the experiment in Ref. [8] the effect of the image attraction is to increase the normal component of the projectile energy by 0.5 eV. We assume that the image attraction is effective only prior to H formation and that it is independent of E_i.

Following Auth and Winter [8], we use the simplified form of the Ziegler-Biersack-Littmark (ZBL) potential

$$U(Z)=a_1\exp\left[-a_2\left(Z-\frac{r_{\rm F^-}}{2}\right)\right], \quad (5)$$

where $a_1=13.9$ eV, $a_2=0.88$ a.u. The radius of the F^- ion in the lattice site $r_{\rm F^-}=2.57$ a.u. [10] appears in Eq. (5) since, in our work, the origin of the reference frame is placed on the first crystal layer (Fig. 1).

The stopping power $-dE/dX(Z)$ has the same functional form as $U(Z)$ in Eq. (5),

$$-\frac{dE}{dX}(Z)=-\frac{dE}{dX}(0)\exp\left[-\frac{a_2}{2}\left(Z-\frac{r_{\rm F^-}}{2}\right)\right], \quad (6)$$

where $-dE/dX(0)=\alpha V_{\rm tg}$, $\alpha=0.177$, and $V_{\rm tg}$ is the tangential component of the projectile velocity given in a.u. For $E_i=5.4$ keV the coefficient $-dE/dX(0)$ is equal to 2.24 eV/a.u. that is close to the value given by Auth and Winter [8] (2.1 eV/a.u.).

The velocity dependence of the stopping power allows a correct reproduction of both the energy [Fig. 2(a)] and angle [Fig. 2(b)] dependences of the projectile energy loss. In Fig. 2(b) we show the projectile energy loss calculated for both exact and simplified ZBL potentials. Following the experiment in Ref. [8], in what follows we present results calculated for fixed $\phi_i=1°$. One can see that the error in the energy loss ΔE due to the use of the potential (5) is very small at this angle. The electron-lattice interaction potential is

$$V_s(\boldsymbol{r})=\sum_{k=1}^{\infty}\sum_{l=1}^{\infty}V_{k,l}(z)f_{k,l}\sin(gkx)\sin(gly), \quad (7)$$

where

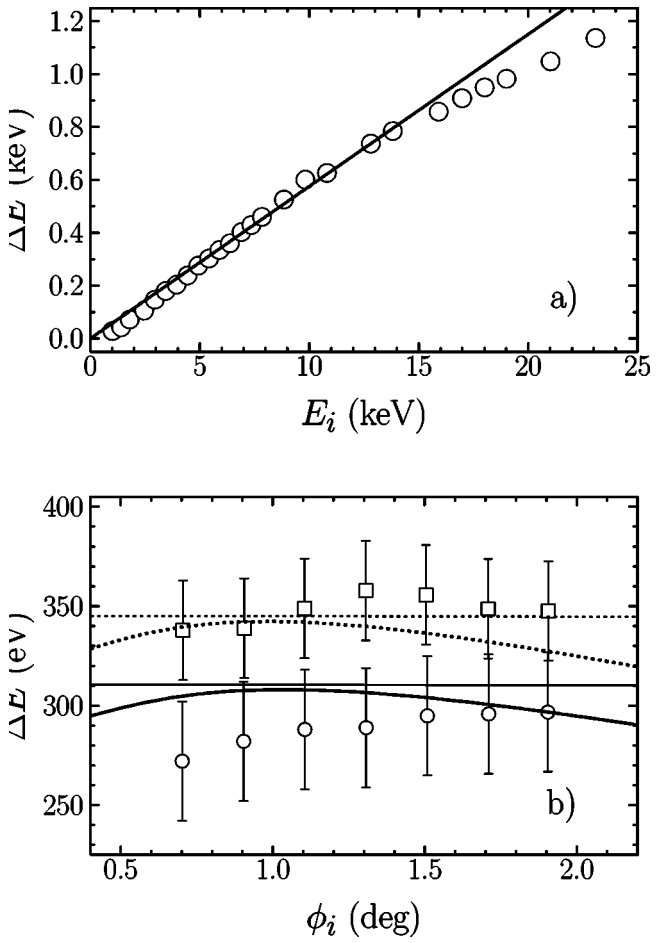

FIG. 2. (a) The projectile energy loss ΔE of H atoms scattered from a LiF surface at a grazing angle $\phi_i = 0.6°$ as a function of initial projectile energy E_i. The solid line is our calculation. The experimental points are taken from Ref. [11]. (b) The projectile energy loss ΔE versus grazing angle ϕ_i for $E_i = 5.4$ keV (circles and solid lines) and 6 keV (squares and broken lines). The thick (thin) lines were calculated using the exact (simplified) ZBL potential. The experimental data are also from Ref. [11].

$$V_{k,l}(z) = \frac{16 \exp(-gz\sqrt{k^2+l^2})}{d\sqrt{k^2+l^2}[1+\exp(-\pi\sqrt{k^2+l^2})]} \tag{8}$$

and

$$f_{k,l} = \frac{\cos[\pi(k-l)/2] - \cos[\pi(k+l)/2]}{2}, \tag{9}$$

and where $g = 2\pi/d$ and $d = 7.6$. We correct the expression for the potential $V_s(\boldsymbol{r})$ given in Refs. [7] and [8] by rederiving the selection factor $f_{k,l}$. In our calculations we only need to retain the following terms of the expansion (7):

$$V_s(\boldsymbol{r}) \approx V_{1,1}(z)\sin(gx)\sin(gy) - V_{1,3}(z)[\sin(gx)\sin(3gy) + \sin(3gx)\sin(gy)]. \tag{10}$$

Note that there is no second-harmonic term $V_{2,2}(z)$ in Eq. (10) since $f_{2,2} = 0$.

The calculated coefficients $a_n(t)$ from expansion (2) can be used to find the Lyman-α radiation intensity. It is proportional to the dipole radiation probability $dW_{i\to f}$ [12],

$$dW_{i\to f} = \frac{\omega^3}{2\pi}|\boldsymbol{n}\times\boldsymbol{d}_{f,i}|^2 d\Omega, \tag{11}$$

where $d\Omega$ is the solid angle, ω is the transition frequency, $\boldsymbol{n}$ is the unit vector in the direction of the light emission, and $\boldsymbol{d}_{f,i} = \langle\varphi_f|e\boldsymbol{r}|\psi_i\rangle$ is the dipole matrix element for the initial state ψ_i described with the postcollision wave function (2) and final state φ_f being the $1s$ state. Taking into account the geometry of the experiment in Refs. [7,8] and substituting Eq. (2) in Eq. (11), one can show that

$$dW_{i\to f} = \frac{8192 e^2 \omega^3}{59\,049\pi}\mathcal{I}_y d\Omega, \tag{12}$$

where

$$\mathcal{I}_y = 2|a_{2,1,0}|^2 + |a_{2,1,-1} - a_{2,1,1}|^2. \tag{13}$$

Note that the time dependence of the wave function ψ_i factors out in the dipole matrix element $\boldsymbol{d}_{f,i}$ after calculation of the squares of the absolute values in Eq. (13).

Under the considered conditions, $\mathcal{I}_y$ is a function of the time-independent y coordinate of the proton through the coefficients a_n of the wave function expansion (2). So the calculated function $\mathcal{I}_y$ is averaged,

$$I_y = \frac{1}{d}\int_{-d/2}^{d/2}\mathcal{I}_y dy, \tag{14}$$

to yield the intensity I_y of the Lyman-α radiation emitted in the y axis direction (arbitrary units are used for I_y in what follows).

III. RESULTS AND DISCUSSION

In this section we analyze the radiation intensity I_y as a function of the initial projectile energy E_i and the switching distance $Z_{\rm sw}$. The calculations were conducted with the use of MATHEMATICA [13].

Figure 3 shows $I_y = I_y(E_i, Z_{\rm tp}(E_i) + \Delta Z)$ as a function of projectile energy E_i and the difference ΔZ between the switching distance $Z_{\rm sw}$ and the energy-dependent distance of the closest approach $Z_{\rm tp}(E_i)$. When calculating I_y, presented in Fig. 3(a), we assumed that switching takes place in the incoming part of the trajectory and hence no quenching allowed. Figure 3(b) illustrates the case where switching occurs after the hydrogen is reflected from the LiF surface. The distinctive feature of these two cases is the behavior of the resonant peak magnitude for large ΔZ. The resonance shown in Fig. 3(a) does not disappear with increasing ΔZ. In fact, for $\Delta Z > 1$ it continues to rise. In the interval $0 < \Delta Z < 2$ the energy dependence of I_y demonstrates a more complicated behavior. It has two local maxima at small nonzero values of ΔZ. The smaller one decreases when ΔZ approaches zero and the major one increases rapidly. In Fig. 3(b) there is only one maximum that peaks at $\Delta Z = 0$. Unlike the earlier case, switching in the outgoing part of the trajectory leads to the intensity magnitude decreasing rapidly with increasing ΔZ.

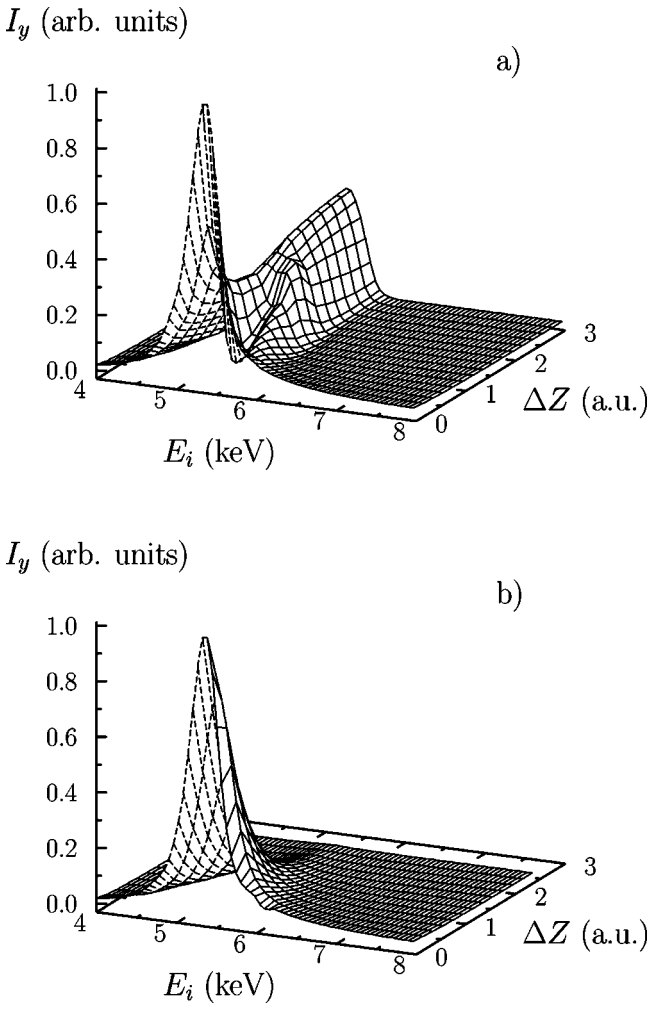

FIG. 3. $I_y = I_y(E_i, Z_{tp}(E_i) + \Delta Z)$, in arbitrary units, versus initial energy E_i and the difference ΔZ for RCE switching occurring in (a) the incoming and (b) outgoing part of the projectile trajectory. $Z_{tp}(E_i)$ is the energy-dependent distance of the closest approach.

Additional information about the dynamical behavior of the system can be extracted from the dependence of the resonance peak position E_{max} on the switching distance Z_{sw}. Figure 4 shows with the solid line the difference ΔE between the peak position E_{max} and the resonance energy $E_{res} = 5.14$ keV $[\Delta E = E_{max}(Z_{sw}) - E_{res}]$ as a function of the switching distance Z_{sw}. Note that here we use constant $Z_{sw} = Z_{tp}(E_i) + \Delta Z(E_i)$, where $\Delta Z(E_i)$ compensates the energy dependence of the turning point $Z_{tp}(E_i)$. Also shown, as a dashed line, is the the energy loss ΔE_{tr} undergone by the atom with initial energy $E_i = E_{max}(Z_{sw})$ up to the switching moment $[\Delta E_{tr} = \Delta E_{tr}(Z_{sw}, E_{max}(Z_{sw}))]$. From Fig. 4 one can see that the shift in the peak position is not equal to the energy loss suffered by the atom when it passes Z_{sw}. Taking into account that the experimentally observed shift is equal to 260 eV, Fig. 4 suggests that the RCE process is switched on at $Z_{sw} = 4$. This is ~ 1 a.u. closer to the surface than it follows if one assumes that the shift is equal to the ΔE_{tr}, as in Ref. [7], for example. Thus, we conclude that the shift in the energy position of the resonant peak is a functional of the projectile trajectory and does not allow a direct determination of the point where the RCE started.

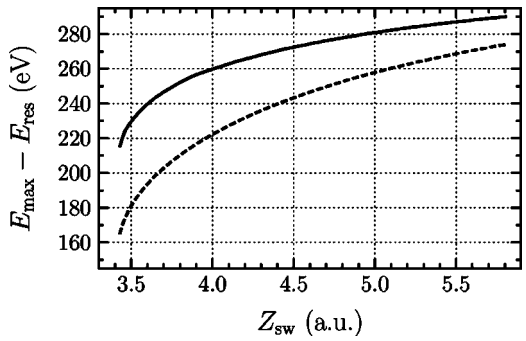

FIG. 4. Peak position E_{max} of the RCE signal $I_y(Z_{sw})$ as a function of switching distance Z_{sw} (solid line). To compare with the energy loss ΔE_{tr} undergone by a projectile with initial energy E_{max} up to the switching moment (dashed line), the origin of the energy axis is moved upward by the resonance energy $E_{res} = 5.14$ keV.

The resonance peak can be moved and its shape altered if the switching distance Z_{sw} is not a constant, but a function of the initial energy $[Z_{sw} \equiv Z_{sw}(E_i)]$. In this work we assume that not only the H formation, but also the quenching of the atom excitation is determined by a mechanism of the charge-exchange type between the projectile and the insulator crystal. In this case one can write the following estimation for Z_{sw} as a function of E_n:

$$Z_{sw}(E_i) = \frac{r_{F^-}}{2} + \frac{1}{\alpha} \ln \frac{\Delta_0}{\alpha v_n(E_i)}, \tag{15}$$

where Δ_0 and α characterize the atomic level broadening in front of the surface and v_n is the normal component of the atom velocity $v_n = [2(E_i \sin^2 \phi_i + E_{im})/M]^{1/2}$ [14]. The energy dependence of the neutralization distance Z_n is of the same functional form as Eq. (15) but with different parameters α and Δ_0.

We use the following guidelines to specify the numerical values for α and Δ_0. For H^+ neutralization, α is assumed to be of the order of the inverse Bohr radius and Δ_0 is of the order of the valence band width. For excited-state quenching, the value of α is to be at least four times less than its value for the case of charge transfer from the LiF valence band to the $1s$ state. It follows from the excited orbital size scaling, which is of the order of n^2 for the nth atomic shell. The numerical value of Δ_0 is chosen arbitrarily since our calculations show it influences only the absolute magnitude of the radiation signal leaving its shape and position unchanged.

Figure 5 presents ΔZ as a function of the initial projectile energy calculated for different models of Z_{sw}. Figure 5(a) illustrates the case where the switching takes place in the incoming part of the trajectory and no quenching is allowed. It shows $\Delta Z(E_i) = Z_n(E_i) - Z_{tp}(E_i)$ where the switching distance Z_{sw} is supposed to be equivalent to the neutralization distance Z_n. To calculate Z_n we use Eq. (15) with $\alpha = 0.7$ and $\Delta_0 = 1.5$ eV. For comparison, we give ΔZ (broken line) calculated for some constant Z_{sw} ($Z_{sw} = r_{F^-}/2 + 3 \approx 4.3$). Its numerical values were chosen to be close to $Z_n(E_i)$ at the energies near the experimental resonance peak position. Fig-

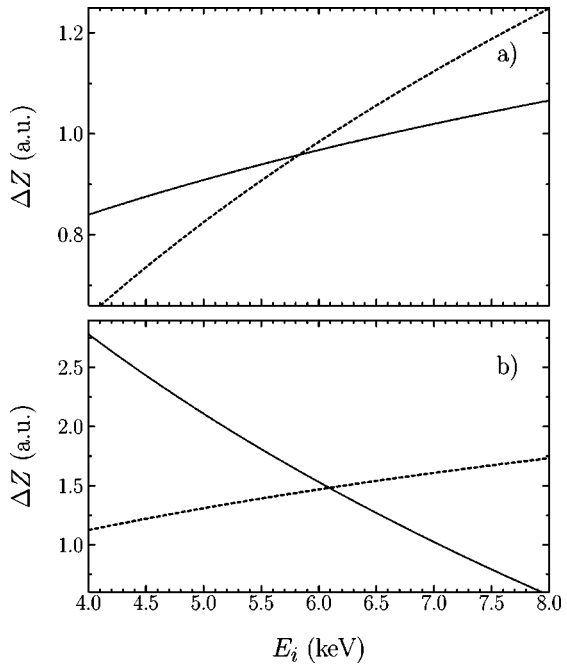

FIG. 5. The energy dependence of $\Delta Z = Z_{sw} - Z_{tp}$ calculated for switching in the (a) incoming and (b) outgoing parts of the projectile trajectory. The solid (broken) line is calculated with energy-(in)dependent Z_{sw}.

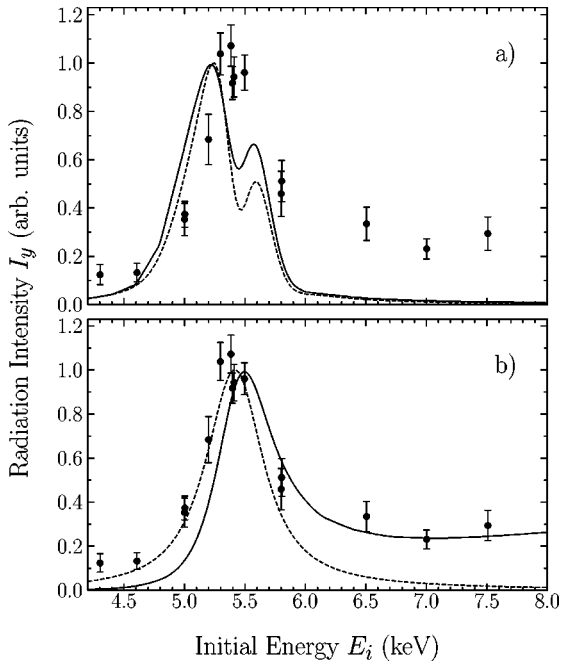

FIG. 6. The normalized RCE signal I_y as a function of projectile energy E_i for the RCE switching in (a) the incoming and (b) outgoing part of the projectile trajectory. The solid (broken) line shows the signal calculated with the use of the energy-(in)dependent switching distance Z_{sw} shown in Fig. 5. The experimental points are taken from Ref. [8].

ure 5(b) shows ΔZ calculated for switching in the outgoing part of the trajectory. The solid line corresponds to ΔZ where $Z_{sw}(E_i)$ is determined by Eq. (15) with $\alpha = 0.095$ and $\Delta_0 = 0.035$ eV. The broken line is calculated for ΔZ with constant Z_{sw} being equal to $r_{F^-}/2 + 3.5 \approx 4.8$. This value of Z_{sw} was used in the paper by Auth *et al.* [7]. Figure 6 shows the energy dependence of the calculated radiation intensity I_y in various models of $\Delta Z(E_i)$ depicted in Fig. 5 and compares with experiment.

The radiation signal I_y calculated for the case of switching in the incoming part of the trajectory is shown in Fig. 6(a). The solid (broken) curve was calculated with the use of ΔZ given in Fig. 5(a) with the solid (broken) line. One can see that the accounting of the energy dependence in Z_{sw} causes insignificant variation of the curve shape, which is unable to explain the experimental background observed for the larger E_i.

The solid (broken) line in Fig. 6(b) was calculated for switching in the outgoing part of the trajectory using the energy-(in)dependent Z_{sw}. We see that the effect of using Eq. (15) is particularly large at the higher energies and allows reproduction of the background signal seen in the experiment. This is due to the fact that with increasing energy E_i the magnitude of the radiation signal [Fig. 3(b)] increases due to the decrease in ΔZ [Fig. 5(b)]. In addition, the position of the peak has moved marginally to higher energies. At the smaller energies the switching distance $Z_{sw} = 4.8$ works better, indicating that the choice (15) can be readily improved to yield agreement with the experiment over the entire energy range. Thus, a suitably chosen $Z_{sw}(E_i)$ is sufficient to describe the observations without the requirement of extra mechanisms as suggested by Auth and Winter [8].

To test the stability of the results presented in Fig. 6 we also conducted calculations for more excited states of atomic hydrogen (including all states with main quantum number $n = 3$) and more terms in the electron-surface potential decomposition (10). These calculations showed negligible deviation from the results presented.

IV. CONCLUSION

We studied the dependence of the resonant coherent excitation (RCE) signal on the switching distance Z_{sw}. This distance separates the region where the excited states of hydrogen cannot survive from the region where the RCE is possible. Contrary to the assumption of Auth *et al.* [7], accounting of the projectile deceleration during excitation showed that the position of the resonant peak is not associated directly with the energy loss undergone by the atom prior to the RCE. In addition, some shift in the peak position can be caused by the energy dependence of the switching distance Z_{sw}. Another consequence of the specified energy dependence is the reproduction of the background observed in the RCE signal at higher energies. The energy dependence of Z_{sw} can be expected, for example, if the quenching of the excited states is caused by the charge-transfer mechanisms from the hydrogen excited states to the LiF conduction band. A quantitative description of this effect demands more sophisticated methods since, generally, the switching distance Z_{sw} can be different for different excited states. The suggested interpretation of the signal background may be further checked experimentally by fixing the component of the projectile velocity v_n normal to the insulator surface. In this

case, Z_{sw} cannot have projectile energy dependence and we expect no background to be observed. We hope that this work will motivate experiments to confirm or reject the suggested interpretation of the presently available measurements.

ACKNOWLEDGMENTS

The work was supported by the Australian Partnership for Advanced Computing. Support of the Australian Research Council is also gratefully acknowledged.

[1] J. Los and J.J.C. Geerlings, Phys. Rep. **190**, 133 (1990).
[2] J. Burgdorfer, in *Review of Fundamental Processes and Applications of Atoms and Ions*, edited by C.D. Lin (World Scientific, Singapore, 1993), pp. 517–615.
[3] H. Winter, J. Phys.: Condens. Matter **8**, 10 149 (1996).
[4] H. Winter, Prog. Surf. Sci. **63**, 177 (2000).
[5] A.G. Borisov and V.A. Esaulov, J. Phys.: Condens. Matter **12**, R177 (2000).
[6] H. Winter, Phys. Rep. **367**, 387 (2002).
[7] C. Auth, A. Mertens, H. Winter, A.G. Borisov, and F.J. Garcia de Abajo, Phys. Rev. Lett. **79**, 4477 (1997).
[8] C. Auth and H. Winter, Phys. Rev. A **62**, 012903 (2000).
[9] P.A. Zeijlmans van Emmichoven, A. Niehaus, P. Stracke, F. Wiegershaus, S. Krischok, V. Kempter, A. Arnau, F.J. Garcia de Abajo, and M. Penalba, Phys. Rev. B **59**, 10 950 (1999).
[10] N.W. Ashcroft and N.D. Mermin, *Solid State Physics* (Holt, Rinehart and Winston, New York, 1976).
[11] H. Winter, C. Auth, and A. Mertens, Nucl. Instrum. Methods Phys. Res. B **164**, 559 (2000).
[12] V.B. Berestetskii, E.M. Lifshitz, and L.P. Pitaevskii, *Quantum Electrodynamics*, Vol. 4 of Course in Theoretical Physics (Pergamon Press, Oxford, England, 1982).
[13] S. Wolfram, *MATHEMATICA, A System for Doing Mathematics by Computer*, 2nd ed. (Addison-Wesley, Redwood City, CA, 1990).
[14] R. Brako and D.M. Newns, Surf. Sci. **108**, 253 (1981).